



**HAL**  
open science

# An Empirical Approach for Mechanical Behavior Characterization of a Small Diameter Cold-Drawn Steel Wire with a Three-Point Bending Test

Julien Vaïssette, Manuel Paredes, Catherine Mabru

## ► To cite this version:

Julien Vaïssette, Manuel Paredes, Catherine Mabru. An Empirical Approach for Mechanical Behavior Characterization of a Small Diameter Cold-Drawn Steel Wire with a Three-Point Bending Test. *Advances on Mechanics, Design Engineering and Manufacturing IV*, Springer International Publishing, pp.1090-1102, 2023, *Lecture Notes in Mechanical Engineering*, 10.1007/978-3-031-15928-2\_95 . hal-03891202

**HAL Id: hal-03891202**

**<https://hal.science/hal-03891202v1>**

Submitted on 12 Dec 2022

**HAL** is a multi-disciplinary open access archive for the deposit and dissemination of scientific research documents, whether they are published or not. The documents may come from teaching and research institutions in France or abroad, or from public or private research centers.

L'archive ouverte pluridisciplinaire **HAL**, est destinée au dépôt et à la diffusion de documents scientifiques de niveau recherche, publiés ou non, émanant des établissements d'enseignement et de recherche français ou étrangers, des laboratoires publics ou privés.

# An empirical approach for mechanical behavior characterization of a small diameter cold-drawn steel wire with a three-point bending test

Julien Vaïssette<sup>1</sup>, Manuel Paredes<sup>1</sup>[0000-0002-5177-4490], Catherine Mabru<sup>1</sup>[0000-0001-6351-9692]

<sup>1</sup> ICA, Université de Toulouse, UPS, INSA, ISAE-SUPAERO, MINES-ALIB, CNRS, 3 rue Caroline Aigle, 31400 Toulouse, France  
lncs@springer.com

**Abstract.** Industrial spring manufacturers have increasingly high production rates with ever finer dimensional requirements. Today, they use tensile tests to evaluate the mechanical behavior of the wires they use to produce their springs. However, this type of test is not easy to handle in an industrial context, because of all the requirements needed for tensile testing, especially when it is done on small diameter wires. Thus, spring manufacturers are interested in replacing the conventional tensile testing by a much simpler and quicker testing. This work proposes an empirical approach for mechanical behavior characterization of small diameter wires, which relies on a three-point bending test and a material isotropy assumption. This approach is designed to fit into an industrial process because it offers a sufficiently accurate characterization of the wires for industrial purpose, and it avoids the biases that can be introduced by the tensile testing method. In this article, this characterization approach was applied to a cold-drawn 0.8mm wire, made of AISI 302 austenitic steel, with very satisfying results.

**Keywords:** Cold-drawn wire, 3-point bending test, characterization approach.

## 1 Introduction

Small diameter wires are widely used in several industries. They can be found in semiconductor packaging [1], electrical conducting wires [2], tire cords, springs, wire ropes and suspension bridge cables [3]. They are therefore produced in extremely large quantities in order to meet the demand. For example, spring manufacturers use spring forming machines that can produce hundreds of thousands of springs per week, with wire feed speed of 121 meter per minute [4]. The direct consequence of this very high production rate is that manufacturers have to meet the demand expectations in terms of both quantity and quality. According to the industry, the quality expectations may vary. However, if we focus only on the spring manufacturers, the quality expectations are very strong: the springs they manufacture are intended to satisfy geometrical, dimensional and mechanical specifications. To achieve these demanding goals, spring manufacturers have to thoroughly characterize the mechanical behavior of the wires they use, in order to find the right settings on their high speed forming machines.

Today, the mechanical behavior characterization is commonly done with tensile testing. This method is a very efficient characterization method since it gives an accurate measure of Young's Modulus, Yield Strength and Ultimate Strength. Moreover, tensile testing is not sensitive to the severe microstructure radial anisotropy of cold-drawn wires as the tensile effort is evenly distributed over the section. Last but not least, tensile testing machines may appear to be very easy to handle and to integrate in an industrial manufacturing process. Right after receiving a coil of cold-drawn wire from a supplier, a spring manufacturer only needs to cut a portion of wire and run the tensile testing machine to get an immediate mechanical behavior characterization of the wire.

However, there are situations when this perfectly seamless characterization process becomes less efficient and accurate: one of those situations is when the wires have small diameter. The first reason why traditional tensile testing becomes less accurate is because the elongation of wires with diameter inferior to 0.2 mm needs to be measured with a more elaborate method than the contact extensometer method [5]. The consequence of this need for adaptation is that it is time consuming, while the industrial process requires a steady level of efficiency to meet the production rate. Spring manufacturers most often decide to lower the quality of their characterization method to keep up the pace of production. But there is another reason why tensile testing loses its accuracy with small diameter wires: the constraints generated by the clamps on the wire can introduce damages on the wire during the testing. Indeed, to avoid the slippery of the wire, the clamps apply pressure which gets closer to the ultimate strength of the material as the diameter lowers. Consequently, small diameter wires break almost immediately after reaching their yield resistance, and the fracture is located at the edge of the clamps (see Fig.1).

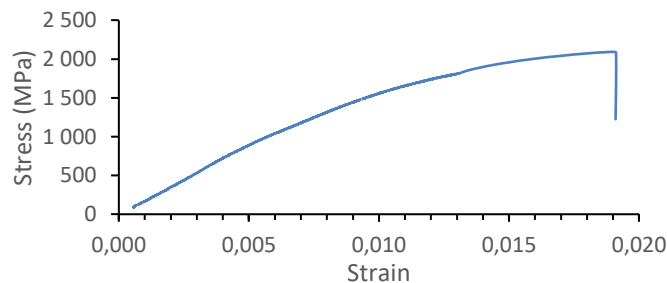


**Fig. 1.** Tensile test curve of a 0.8 mm wire.

This early fracture during tensile testing prevents spring manufacturers from having a comprehensive idea of the mechanical behavior of the wire they will form. They miss a significant part of the plastic behavior of their wire. This lack of accuracy during tensile testing leads to a greater scrap rate of their forming machines. To avoid this situation, spring manufacturers often use capstan-type grippers that consists of winding the wire around grippers. This lowers the stress concentration but it is also time consuming as it requires more preparation than traditional tensile testing. If we add that this adaptation is not sufficient for achieving a good reliability because it does not solve the problem of measuring elongation (which stays equally hard on small diameter wires

with this method), we understand that spring manufacturers need a simpler solution to characterize the mechanical behavior of their small diameter wires. This work explores a characterization method for small diameter wires, which relies on a three-point bending test with both numerical and experimental approaches. All spring manufacturers have machines to test the axial behavior of springs that can be easily exploited to perform three-point bending tests [6-7] (which was preferred over the four-point bending test because it is easiest to handle in a manufacturing context). Moreover, the three-point bending test is not sensitive to the wire diameter, since there is less stress concentration. It was therefore decided to verify the relevance of the three-point bending test in order to characterize wires which diameter is less than 1 mm. In this context, it is preferable to work with a simplifying hypothesis of material isotropy. This paper will show that the results obtained with this strong assumption [8] are still very satisfying.

## 2 Experimental and numerical details

### 2.1 Materials and testing

The material selected for this work is an austenitic steel wire whose diameter is 0.8 mm and its steel grade is AISI 302. According to the European Standard NF EN 10270-3 [9], its Young's Modulus is 185 GPa (heat treated) and its ultimate resistance is between 2100 and 2415 MPa. In other words, when spring manufacturers receive this wire, they only have a vague knowledge of the mechanical characteristics of the wire, since the European Standard gives very limited information and tensile testing obliterates a large portion of the plastic behavior of the wire. The three-point bending test bench (see Fig. 2) used in this study is the automatic Andilog Stentor II 5000 bench (0.1 mm accuracy per 300 mm travel). The loading pin is connected to a 50N sensor (0.05 N accuracy). The test bench directly includes 5 different sets of supporting pins in order to enable tests of a large range of wire diameters without additional tuning. For the studied wire of 0.8mm diameter, the first set of the supporting pins is selected. The supporting pins were separated by a distance of 22.3 mm. The diameter of the pins is 3 mm.

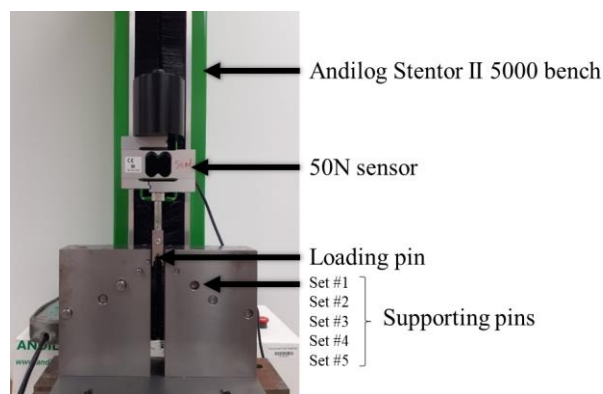


**Fig. 2.** The experimental bench.

## 2.2 Numerical modeling

Finite Element calculations were carried out to simulate three-point bending tests. The simulation model was designed to simulate the three-point bending test with the most precise accuracy with an extremely fine mesh (the element size was 0.067 mm). The simulation software used for this work is Abaqus in quasi-static with non-linear geometry, with the following boundary conditions: longitudinal symmetry on the loading pin, the center of the loading pin is fixed, longitudinal symmetry on the wire and radial symmetry on the wire at contact point with the loading pin. Unlike in the experimental test, the supporting pin moves and applies the deformation to the wire. The interaction properties between the two pins and the wire allow finite sliding, and are “hard contact” interactions (see Fig. 3).

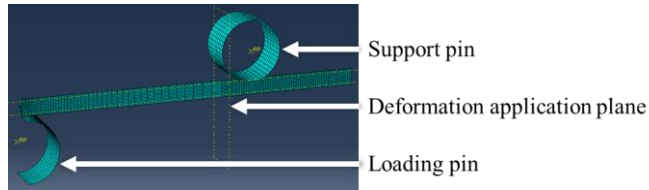


Fig. 3. The Finite Elements model of the three-point bending test.

## 3 Methodology

### 3.1 Experimental and numerical bending tests

The initial idea is to replace tensile testing by three-point bending testing. Consequently, this approach must provide the same information on the mechanical characteristics of the small diameter wires as tensile testing. In short, this approach has to estimate a tensile stress-strain curve using a bending curve. To meet this expectation, the objective is to find the simplest way to go from a bending curve to a stress-strain curve. The first step consists in performing a three-point bending test on a 0.8mm diameter wire.

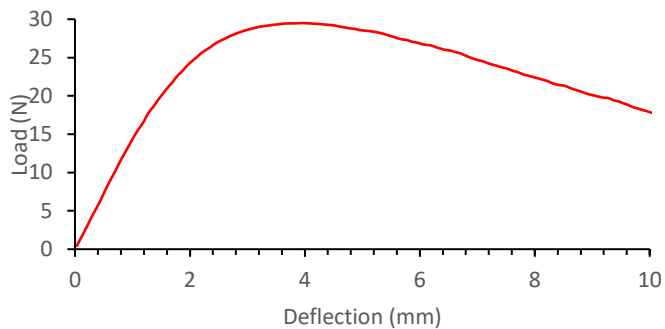
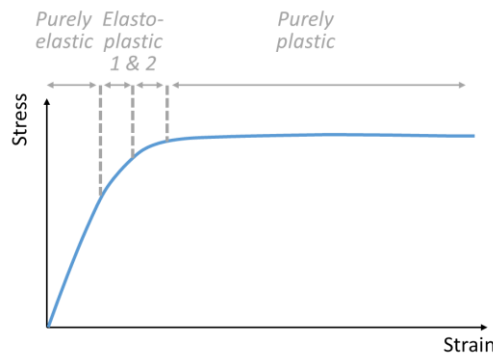


Fig. 4. Example of three-point bending curve obtained on the 0.8mm cold-drawn wire

Thanks to this test, a bending curve is obtained that plots the loading resistance of the wire against the deflection (see Fig. 4). This bending curve can be seen as the input information of this mechanical behavior characterization approach. The next step is to notice that small diameter cold-drawn wires have stress-strain curves that are essentially composed of four linear portions: the purely elastic portion at the beginning of the curve, the purely plastic portion at the end of the curve and two elastoplastic portions forming a triangle shape between the two portions mentioned before (see Fig. 5). Estimating a four linear portion curve means estimating the position of three special points. The first one is the point that marks the end of the purely elastic portion, known as Yield Strength. The second one is the point that marks the start of the purely plastic portion, known as the ultimate resistance. The last one is the middle point, which is described in this work as the “elastoplastic point”. In order to estimate the position of these three points, it is therefore needed to identify three points on the bending curve, each one leading to its corresponding point on the stress-strain curve. The three remarkable points on the bending curve are defined as follows.



**Fig. 5.** The traditional stress-strain curve with four pseudo-linear portions [10].

**The end of the linearity point.** This point is reasonably easy to measure, since it marks the end of the first linear portion. However, a challenge lies in the end of the linearity criterion, and by induction, in the linearity criterion. Indeed, determining a linearity criterion by geometrical interpretation is always difficult. To perform this, the best solution is to proceed by numerical simulation. With the three-point bending test simulation model that was previously described and the exact same parameters that the experimental test performed before (diameter of the wire, of the pins, distance between the pins and isotropy hypothesis), a bending curve can be drawn. The next step is to reverse engineer the linear criterion needed, because the elastic parameters we must geometrically read are already known, since they are entered as an input of the simulation (Yield Strength, Young’s modulus). The input parameters of this simulation were chosen to achieve a bending curve very close to the bending curve obtained experimentally. The input parameters are given in Table 1.

**Table 1.** Input parameters.

Stress (MPa)	Plastic Strain	Young's Modulus (GPa)	Poisson's Ratio
1000	0	165	0.28
1811	0.004		
2200	0.024		

With this method, it was discovered that the best linear criterion is to gauge the linearity of the points of the curve with the Pearson correlation coefficient  $r^2$  from the first point of the curve. The end of the linearity is marked by the point whose  $r^2$  goes under 0.9995. With this method, the geometrically estimated Elastic Modulus is 164 GPa, according to formula (1), calculating the bending elastic modulus [11]. And the elastic modulus is evaluated from the bending curve obtained experimentally at about 166 GPa. It is important to underline that this bending modulus is significantly inferior to the elastic modulus stated by the European Standard of 185 GPa. This gap can be explained by the material anisotropy of the cold-drawn wire. Indeed, the difference between bending and Young's Modulus of anisotropic materials is well documented [12] in the scientific fields where anisotropic materials are common. As the radial anisotropy of cold-drawn wires (especially small diameter cold-drawn wire, with their strong reduction ratio) is also well documented [8], the difference between the measured bending elastic modulus and the Young's Modulus of the wire is not a surprise. However, it was decided to rely on the hypothesis of the isotropy of the wire studied in this work. It is consequently assumed that the measured bending modulus is equal to the Young's Modulus of the wire. To measure the end of the linearity point, it was decided to draw a line parallel to the linear portion identified before, offset by 0.036 mm. This offset was chosen because it was equal to 0.1% of the deflection of the maximum load point. The end of the linearity point is at the intersection of this line with the bending curve. Its coordinates are thus 0.96 mm and 13.77 N.

$$E = \frac{F L^3}{\Delta 48 I} \quad (1)$$

Where: F is the vertical load applied by the loading pin in N; L is the distance between the two supporting pins in mm; I is the inertia moment of the section with respect to the vertical axis in  $\text{mm}^4$ ;  $\frac{F}{\Delta}$  is the slope measured with the linearity criterion in  $\text{Nmm}^{-1}$ ; E is the bending elastic modulus in MPa.

**The maximum load point.** This point is easy to measure: it is only needed to read the maximum load of the bending curve, which is 29.5 N on the bending curve experimentally drawn. The deflection corresponding to this maximum point is read by calculating the mean deflection of the portion of the curve where the load is superior to 99% of 29.5 N. This allows mitigating the risk of an inaccurate reading of the maximum load point. The maximum load point is thus located at a 3.95 mm deflection.

**The intermediate point.** After several iterations, it was found that this point must be measured at the intersection of the bending curve and a line starting from zero, with a

slope equal to 86% of the slope of the first linear portion. On the bending curve experimentally drawn, this point is located at the coordinates 1.88 mm and 23.31 N.

### 3.2 From a bending curve to a stress-strain curve

Once the three remarkable points are measured on the bending curve, this approach translates these points into the three remarkable points of a stress-strain curve. As a reminder, these three remarkable points are: Yield Strength, elastoplastic point and ultimate resistance. At this point, the only known parameter is the Young's Modulus, which is estimated at 166 GPa. It therefore remains for us to calculate the coordinates of the three remarkable points of the stress-strain curve.

**Yield Strength.** In order to translate the end of the linearity point that was previously measured (0.96 mm and 13.77 N) into Yield Strength, the maximum stress associated with this point of the bending curve is calculated as follows (2).

$$\sigma_f = \frac{8FL}{\pi d^3} \quad (2)$$

Where:  $d$  is the diameter of the wire in mm;  $\sigma_f$  is the maximum stress MPa.

Thanks to equation (2), the maximum stress located at the surface of the wire is calculated at 1527 MPa. One could think that Yield Strength is equal to 1527 MPa. It is not: by doing the same calculation with the bending curve obtained by numerical simulations, the flexural stress calculated from the end of the linearity point is 1721 MPa, while the model was set with a 1000 MPa Yield Strength. There is obviously a difference between the apparent Yield Strength value (meaning the stress calculated at the surface of the wire at the end of the linearity point of the bending curve) and the real Yield Strength value. In the case of the numerical simulation of the 1000 MPa Yield Strength wire, the ratio is 1.721/1. To ensure that this ratio between apparent and real Yield Strength was maintained, independently of the Yield Strength that was set up in the model.

Therefore, 12 other simulations of three-points bending tests were carried out, with the exact same parameters, except for Yield Strength. The tested Yield Strength values are as follows: 800 MPa, 850 MPa, 900 MPa, 950 MPa, 1050 MPa, 1100 MPa, 1150 MPa, 1200 MPa, 1500 MPa, 1600 MPa, 1700 MPa and 1900 MPa (this last Yield Strength value implies that there is no elastoplastic point on the stress-strain curve). It appears that the ratio is not constant for all the tested values (see Fig. 6), but it tends to follow a second-degree polynomial distribution.



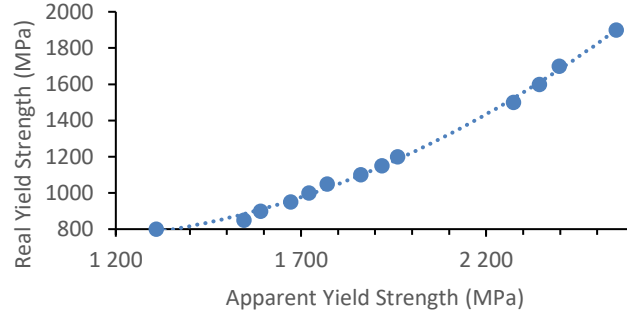


**Fig. 6.** The evolution of the relation between apparent Yield Strength and real Yield Strength.

This second-degree polynomial distribution is described by formula (3), with a Pearson's coefficient of over 0,997. With this formula, the real Yield Strength was estimated for all 12 numerical simulations, with a precision ranging from -2% to +4%. The accuracy of this formula was verified with three other numerical simulations, setting up random values of Yield Strength (919 MPa, 1085 MPa and 1257 MPa). The apparent Yield Strength was measured for each bending curve and formula (3) was used to estimate the real Yield Strength values. Again, the results were satisfying, with very reasonable errors (ranging from -0.1% to +0.6%). With these controls, the accuracy of this Yield Strength estimation formula is quite good, at least in the case of 0.8 mm diameter wires. Formula (3) allows to estimate that the experimentally tested wire has a 874 MPa Yield Strength value.

$$\sigma_s = 4.7812 \times 10^{-4} \sigma_{s\_app}^2 - 9.7844 \times 10^{-1} \sigma_{s\_app} + 1.2070 \times 10^3 \quad (3)$$

Where:  $\sigma_s$  is the real Yield Strength in MPa;  $\sigma_{s\_app}$  is the apparent Yield Strength in MPa.

**Elastoplastic point.** From the intermediate point measured on the bending curve at 1.88 mm and 23.31 N, it is possible to estimate the location of the elastoplastic point of the stress-strain curve (the one that connects the two linear elastoplastic portions of the curve, between the purely elastic and the purely plastic portions). As it is located close enough to the end of the linearity point, it was decided to make the assumption that this point is still in the elastic behavior portion. With this hypothesis, the tensile stress corresponding to this point can be calculated with formula (3), with the same operating mode as for the Yield Strength estimation. With this assumption, the elastoplastic point matches a 1952 MPa stress value. Concerning the strain value of elastoplastic point, it is necessary to moderate the strong hypothesis on which relies the estimation of the stress corresponding to the elastoplastic point with the estimation of the strain corresponding to this same point. To do so, the Yield Strength that would correspond to the same deflection as the one of the intermediate point (1.88 mm) is derived with the hypothesis of purely elastic behavior. The elastic portion line is thus extended up to 1.88 mm. To this abscissa, the line matches a 27.04 N load, which corresponds to a 2999

MPa apparent Yield Strength and a 2664 MPa real Yield Strength. With this result, it can be concluded that the 1952 MPa estimation of the elastoplastic stress value is equivalent to 73% of the purely elastic stress for the same deflection of 1.88 mm. This ratio allows us to estimate a value of the apparent elastic modulus, which is equal to 73% of the elastic modulus of the wire. By doing so, the Hooke's Law that specifies the elastic behavior of a material can be used. With this assumption of pseudo-elasticity, the elastoplastic point can be located at the coordinates 1952 MPa and 0.016:

$$E' = E \times \frac{\sigma_{elastoplastic}}{\sigma_{elastic}} \quad (4)$$

Where:  $\varepsilon_{elastoplastic}$  is the elastoplastic point corresponding strain;  $\sigma_{elastoplastic}$  is the elastoplastic point corresponding stress in MPa (1952 MPa in the case of the experimentally tested wire);  $E$  is the elastic modulus of the elastic portion of the bending curve in MPa (166 GPa here);  $\sigma_{elastic}$  is the stress calculated at the intermediate point deflection, with the assumption of pure elastic behavior, in MPa (2664 MPa here).

**Ultimate strength.** The ultimate strength is estimated with regard to two remarks that can be made at the sight of the numerical simulations described earlier. The first is that the ultimate strength stress value is proportional to the deflection position of the maximum load point of the bending curve, when all the other points of the stress-strain curve are unchanged. Indeed, 22 numerical simulations of three-points bending tests were performed, where the only varying parameter was the position of the ultimate strength point, with a linear distribution of the points measured (see Fig. 7).

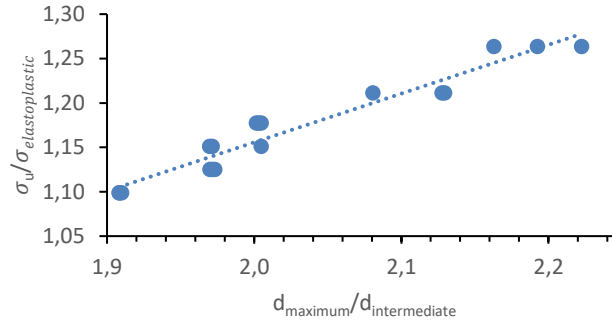


**Fig. 7.** The linear evolution of the ultimate strength depending on the deflection at the maximum load point of the bending curve, obtained with 22 numerical simulations where the only changing parameter was the ultimate strength position.

The linear evolution is described by the formula (5). On the bending curve that was drawn for the wire studied in this work, the  $d_{\text{maximum}}/d_{\text{intermediate}}$  ratio is 2.10 mm. The ratio  $\sigma_u/\sigma_{\text{elastoplastic}}$  is thus derived to be 1.21, corresponding to an ultimate strength of 2366 MPa.

$$\frac{\sigma_u}{\sigma_{\text{elastoplastic}}} = 0.5492 \frac{d_{\text{maximum}}}{d_{\text{intermediate}}} + 0.0572 \quad (5)$$

Where:  $d_{maximum}$  is the deflection of the maximum load point on the bending curve in mm;  $d_{intermediate}$  is the deflection of the intermediate point on the bending curve in mm;  $\sigma_u$  is the ultimate strength in MPa.

Finally, the ultimate strength deflection is estimated thanks to an abacus created for this work, based on the 22 numerical simulations conducted. Indeed, the 22 simulations were made with three variations of second elastoplastic portion slope, which seems to be responsible for the maximum load of the bending curve. These three slopes were calculated as a function of the elastic modulus. 7 simulations were made with a second elastoplastic portion slope equal to 6.76% of the elastic modulus, 7 simulations with a second elastoplastic portion slope equal to 9.04% of the elastic modulus and 8 simulations with a second elastoplastic portion slope equal to 11.00% of the elastic modulus (see Fig.8). As it is possible to locate the  $\sigma_u/\sigma_{elastoplastic}$  ratio at 1.21 and the maximum load over intermediate load at 1.27, the slope of the second elastoplastic portion of the stress-strain curve of the wire studied in this work can be calculated: 5.6% of 166 GPa, which corresponds to a 9250 elastic modulus, and leads to an ultimate strength strain of 0.0608. This marks the end of the stress-strain curve estimation. Table 2 sums up the parameters obtained with the approach explained in this paper.

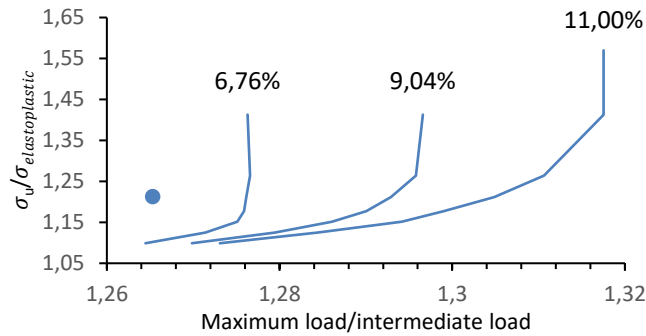


**Fig. 8.** The abacus allows estimating the slope of the second elastoplastic portion of the stress-strain curve, as a function of the elastic modulus.

**Table 2.** The estimated stress-strain curve parameters.

Stress (MPa)	Total Strain	Young's Modulus (GPa)
874	0.0053	166
1952	0.0160	
2366	0.0608	

## 4 Results and discussions

To ensure the validity of this approach of the stress-strain curve estimation from a bending curve, the reverse path was taken: a simulation of the three-point bending test

was performed with the parameters seen in Table 2. The numerical estimated bending curve obtained (see Fig. 9) was then compared with the one experimentally obtained. It can be seen that the bending curve obtained by numerical simulations with this mechanical behavior characterization approach is very close to the experimental bending curve. More precisely, the maximum load point is located at 29.75 N (+0.83% error) and 3.88 mm (-1.80% error). However, this curve is only a proof that this empirical approach is calibrated for the experimentally tested wire. To verify if this approach gave good results on other three-points bending tests, the exercise was made with a wire of the same diameter and same steel grade, but of a different batch. The idea was to confront this approach with a bending curve sufficiently different (see Fig. 10).

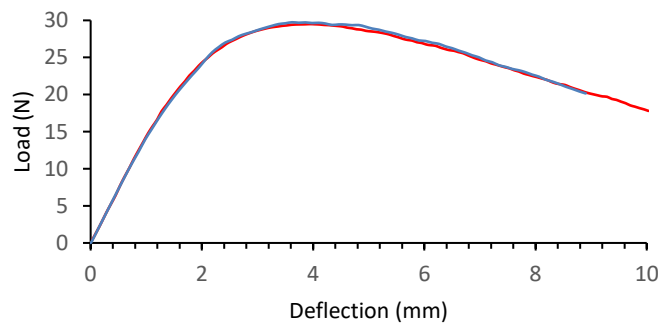


**Fig. 9.** The experimental bending curve is red and the numerical bending curve is blue.

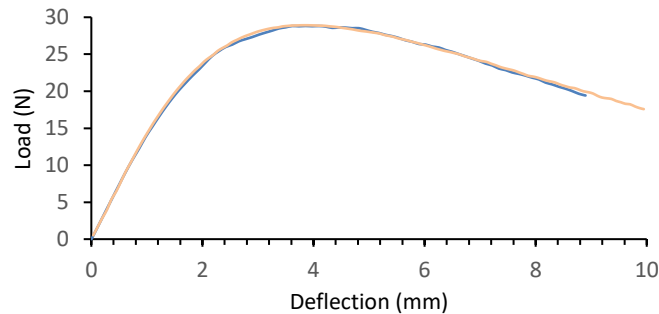


**Fig. 10.** The experimental bending curve is orange and the numerical bending curve is blue (Input parameters: Young's Modulus 167 GPa ; coordinates of the 3 remarkable points: 811 MPa, 0.0049 total strain; 1755 MPa, 0.0143 total strain; 2226 MPa, 0.0408 total strain).

The orange curve is sufficiently different from the red curve (28.92 N maximum against 29.5 N) but the estimation of the stress-strain curve gives a bending curve which is really close to the rose curve: 28.83 N (-0.33% error) and 4.04 mm (+3.40% error) for the maximum point. This approach seems to give a precise indication of the stress-strain curve we might expect from a wire, with a simple and quick three-point bending test. However, this approach was ran with wires of different diameters, and it obtained poor results (the elastic behavior was well predicted but the plastic behavior was not). The reasons for this divergence was investigated, and it was found that it is mostly

caused by the formula (3), giving the real Yield Strength. Indeed, the distribution of the real Yield Strength over the apparent Yield Strength is highly determined by the diameter of the wire. This problem can be solved by running numerical simulations for a large number of wire diameters, in order to give the right formulas to go from the three remarkable points of the bending curve to those of the stress-strain curve.

## 5 Conclusion

As a conclusion, this work shows that it is possible to have an accurate idea of the mechanical behavior of a small diameter wire without needing a complicated tensile machine. This work shows that it is possible to estimate with a fine level of precision (up to only 3.40% error on the bending curve numerically obtained) the stress-strain curve of a wire, allowing every spring manufacturer to better understand the mechanical characteristics of the wire they use. To summarize, the idea is to pick three remarkable points on a three-point bending curve and to translate them into three remarkable points of a stress-strain curve. Moreover, to improve accuracy of our approach for a given manufacturing process, one calibration procedure from a tensile test can be performed on the wire of the very first wire spool and only one rapid bending test is required on each following spool to evaluate potential variations of wire material properties. This approach is promising, because it is widely quicker to use for the manufacturer. Of course, it needs to be explored wider for better accuracy and better versatility.

## References

1. Cho, J.H., Kim, Y.W., Oh, K.H. et al. Recrystallization and grain growth of cold-drawn gold bonding wire. *Metall Mater Trans A* 34, 1113–1125 (2003).
2. X Sauvage, L Renaud, B Deconihout, D Blavette, D.H Ping, K Hono, Solid state amorphization in cold drawn Cu/Nb wires, *Acta Materialia*, Volume 49, Issue 3 (2001).
3. Liu, Shi Feng, et al., Studies of Annealing Process in Severely Cold Drawn Pearlitic Steel Wires, *Materials Science Forum*, vol. 682, Trans Tech Publications, Ltd. (2011).
4. Baudrand New Tech.
5. Gondo, S., Suzuki, S., Asakawa, M. et al. Establishing a simple and reliable method of measuring ductility of fine metal wire. *Int J Mech Mater Eng* 13, 5 (2018).
6. Afnor, Plastics – Determination of flexural properties, NF EN ISO 178 (2019).
7. J. S. Stölken and A. G. Evans, A microbend test method for measuring the plasticity length scale, *Acta Materialia* (1998).
8. J Toribio, F.J Ayaso, Anisotropic fracture behaviour of cold drawn steel: a materials science approach, *Materials Science and Engineering: Volume 343, Issues 1–2* (2003).
9. Afnor, Steel wire for mechanical springs - Part 3, NF EN 10270-3 (2001).
10. Carole Levrau. Compréhension et modélisation des mécanismes de lubrification lors du tréfilage des aciers inoxydables avec des savons secs. *École Nationale Supérieure des Mines de Paris* (2006).
11. Petrescu, Irina Elena, Cristina Mohora, Constantin Ispas. The determination of young modulus for CFRP using three point bending tests at different span lengths, *U.P.B. Sci. Bull* (2013).
12. Spatz H., Vincent J., Young's moduli and shear moduli in cortical bone, *Proc. Lond.* (1996).